

## Supporting Information

### ***'Bio-inspired'* Carbon Hole Extraction Layer Derived from Aloe Vera Plant for Cost Effective Fully Printable Mesoscopic Perovskite Solar Cells**

*Sawanta S. Mali, Hyungjin Kim, Jyoti V. Patil and Chang Kook Hong\**

*\*Polymer Energy Materials Laboratory, School of Advanced Chemical Engineering,  
Chonnam National University, Gwangju, S. Korea-500757,  
Email: swanta@jnu.ac.kr (SSM), hongck@jnu.ac.kr (CKH)\**

**Fig. S-1** Thermogravimetric analysis (TGA) curves of as synthesized (black solid line) and annealed (red solid line) at 1000 °C AV-C powder sample.

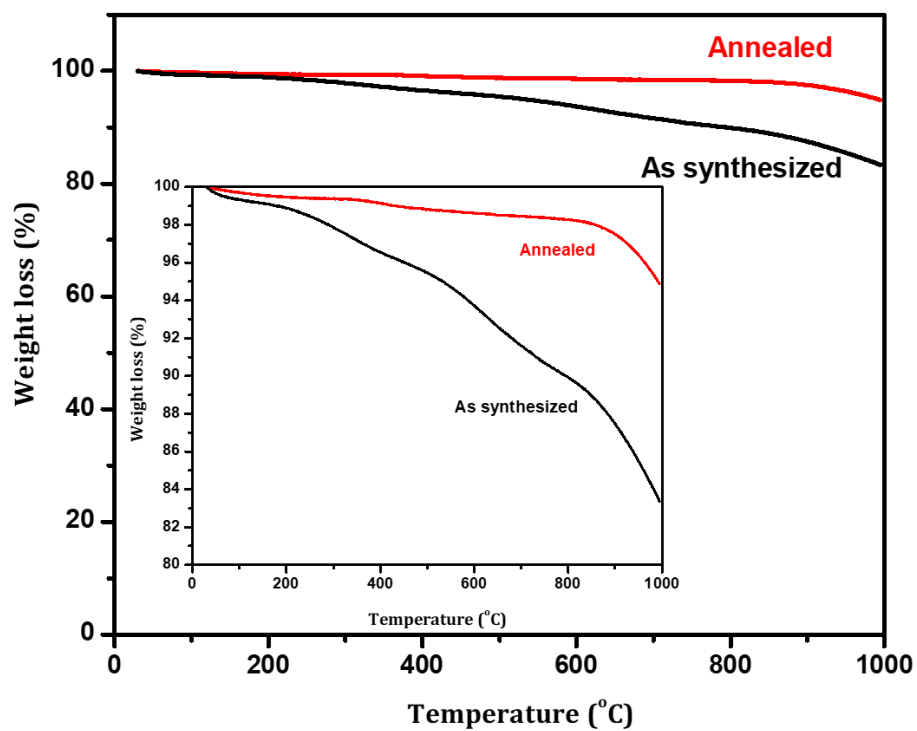


**Fig. S-2 Surface morphology of screen-printed commercial colloidal carbon and bio-inspired AV-C after 12 hours' ball milling** (a) top-view of screen printed commercial colloidal carbon (b) top-view screen printed AV-C and (c-e) TEM and HRTEM images of AV-C after ball milling for 12 hours at different magnification.

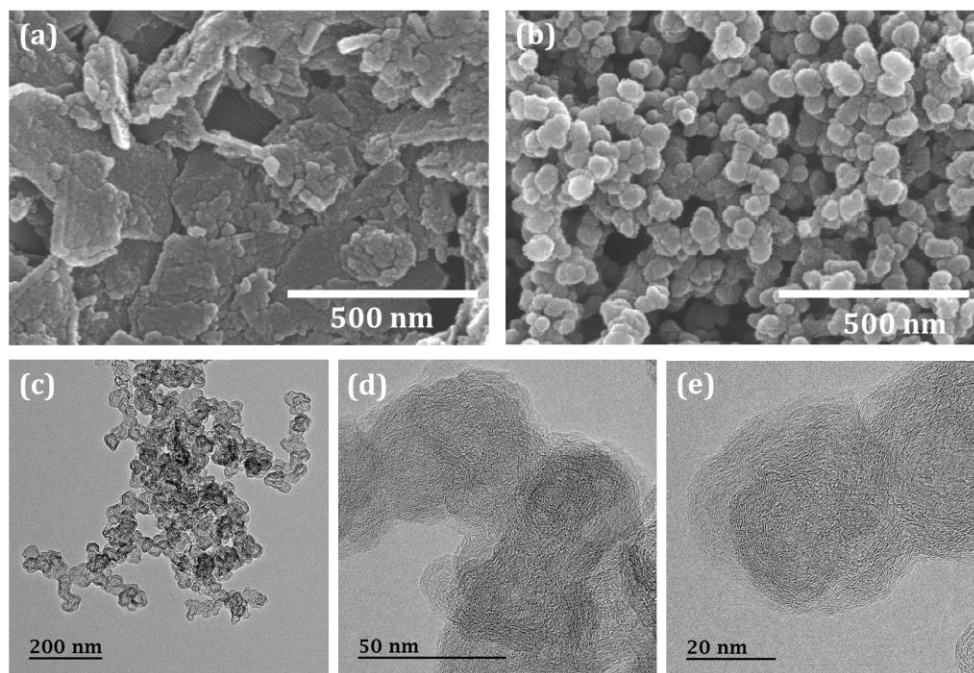
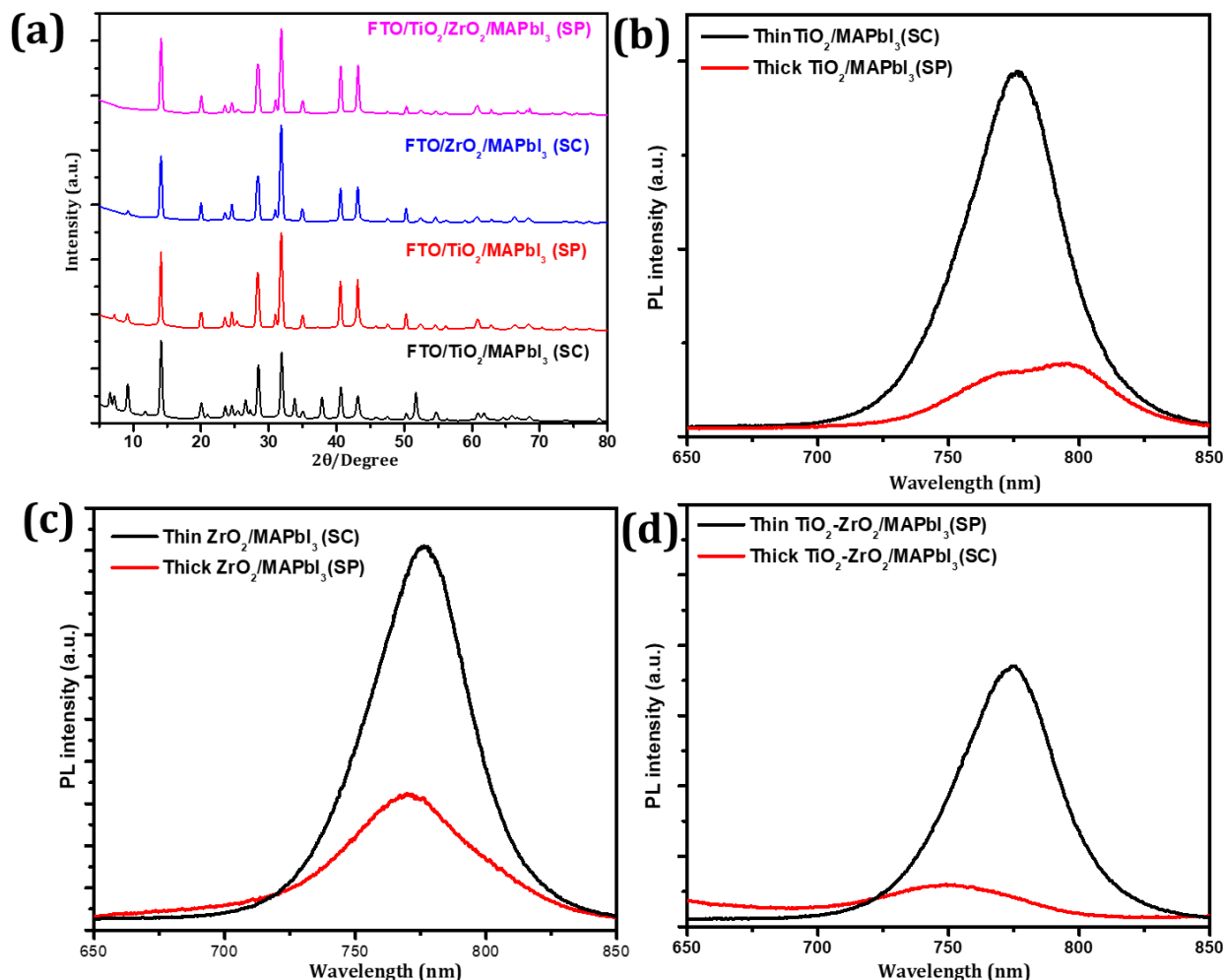


**Fig. S-3** (a) XRD spectra MAPbI<sub>3</sub> deposited on different substrate. Note: SP: screen printed TiO<sub>2</sub> or ZrO<sub>2</sub>; SC: spin coated TiO<sub>2</sub> or ZrO<sub>2</sub> and (b) normalized PL spectra of MAPbI<sub>3</sub> perovskite deposited on thin (black solid line) and thick (red solid line) TiO<sub>2</sub> mesoporous oxide (c) normalized PL spectra of MAPbI<sub>3</sub> perovskite deposited on thin (black solid line) and thick (red solid line) ZrO<sub>2</sub> (d) normalized PL spectra of MAPbI<sub>3</sub> perovskite deposited on thin (red solid line) and thick (black solid line) TiO<sub>2</sub>-ZrO<sub>2</sub> bilayers. All PL spectra were recorded with excitation from perovskite side.



**Discussion Supplementary Fig. S-3:** The structural properties of MAPbI<sub>3</sub> perovskite deposited on different oxide layer was analyzed by XRD measurements. In order to avoid the peak from AV-C we have recorded the XRD spectra only for perovskite layer deposited/infiltrated onto either mp-TiO<sub>2</sub>, ZrO<sub>2</sub> or both oxide samples. The infiltrated or spin coated sample was further annealed at 50 °C for 1h and used for measurements. The XRD spectrum of mp-TiO<sub>2</sub>/perovskite exhibits the strong peak at 2θ=14.1° which can be assigned (110) of MAPbI<sub>3</sub> crystal. All samples show strong peak at 14.1° which clearly exhibited formation of highly crystalline MAPbI<sub>3</sub> layer. Figure S-3b shows the PL spectra of MAPbI<sub>3</sub> deposited on thin and thick mp-TiO<sub>2</sub> which clearly shows double around 750-830 nm. Similar observation has been observed for ZrO<sub>2</sub>/ MAPbI<sub>3</sub> sample however there is no doublet form may be due to front illumination. In case of TiO<sub>2</sub>/ZrO<sub>2</sub>/ MAPbI<sub>3</sub> sample the intensity of screen printed sample reduced drastically which clearly revealed the proper infiltration of MAPbI<sub>3</sub> solution and formation of crystalline MAPbI<sub>3</sub> crystal.

**Fig. S-4 (a)** XRD spectra MAPbI<sub>3</sub> and MAPbI<sub>3-x</sub>Cl<sub>3</sub> deposited on FTO substrate.

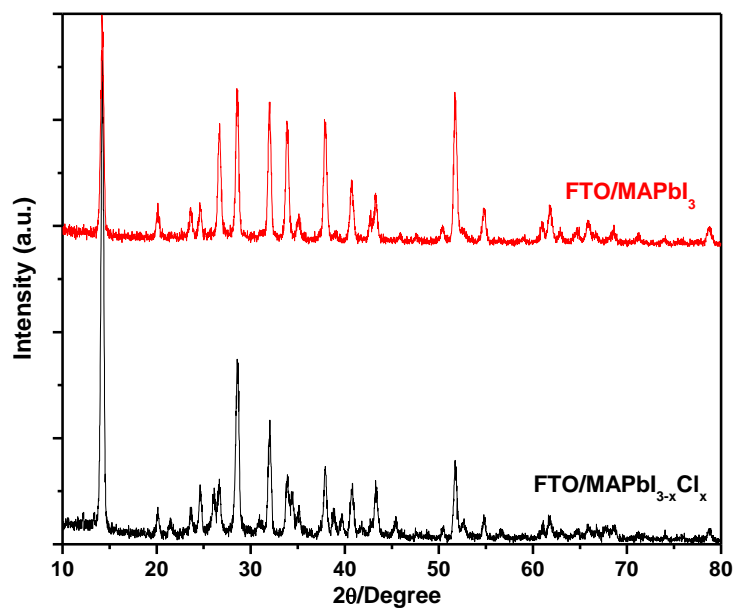
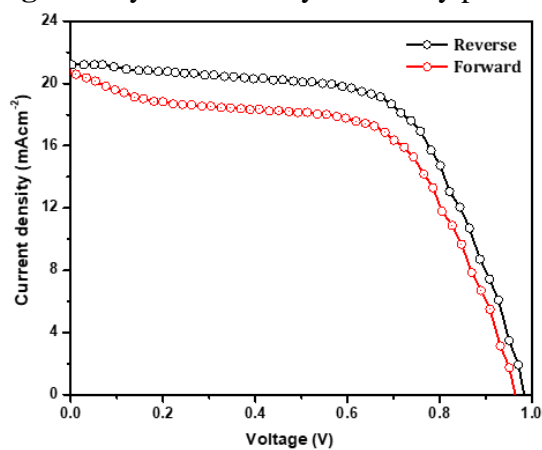


**Fig. S-5** Hysteresis analysis of fully printable AV-C based PSC



Scan	F	R
V <sub>OC</sub> (V)	0.961	0.985
J <sub>SC</sub> (mAcm <sup>-2</sup> )	20.85	21.22
FF	57 %	61 %
Eff. (%)	11.42	12.75

**Fig. S-6** EDS-line mapping of FTO/Bi-TiO<sub>2</sub>/(mp-TiO<sub>2</sub>/ZrO<sub>2</sub>)+MAPbI<sub>3</sub>/carbon PSC (a) artificially colored cross sectional SEM graph of device (b, c) line profile of all elements (d) EDS line scanning profile of each element across the device from bottom-to-top (e) respective EDS spectrum

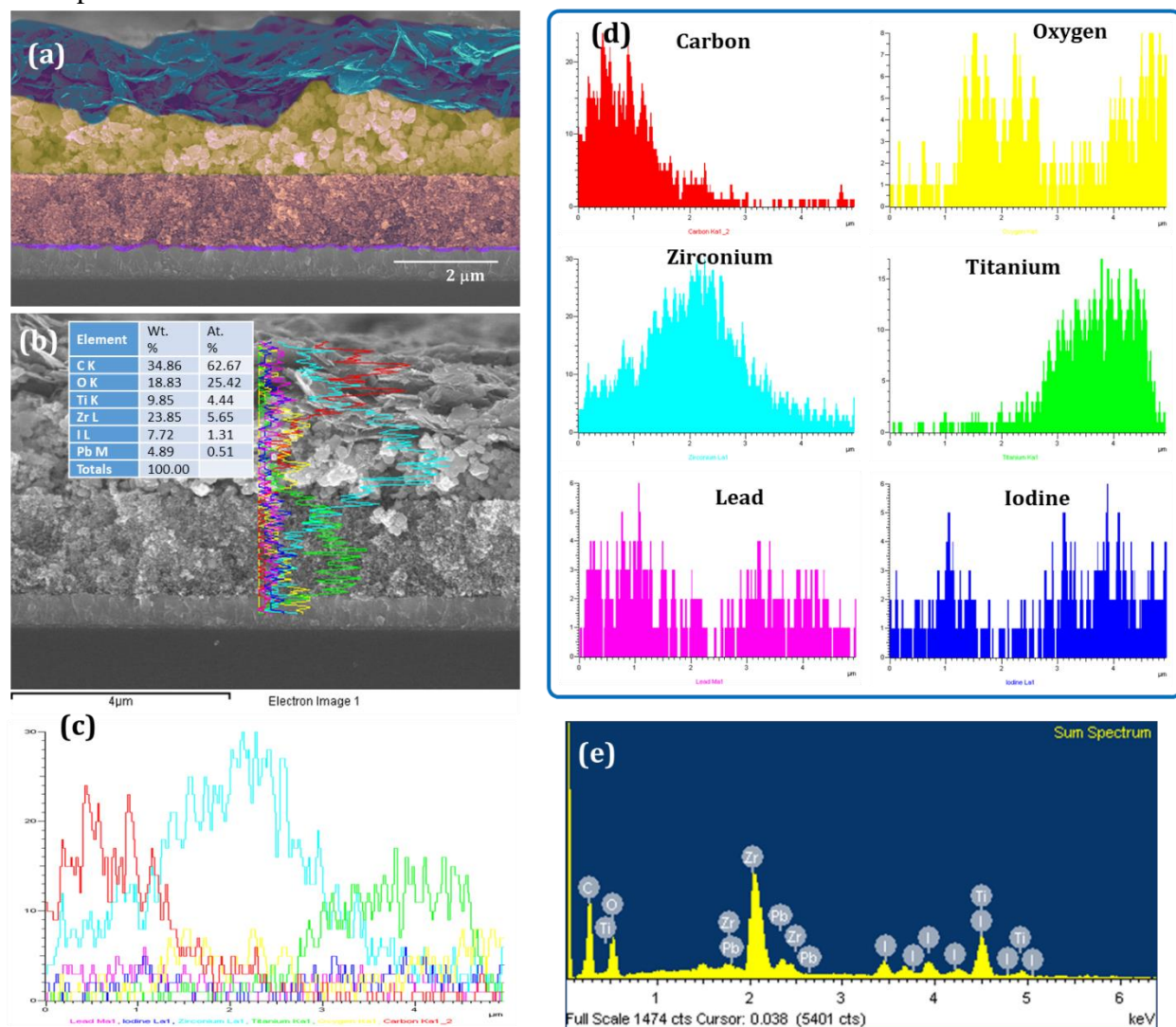


**Fig. S-7** EDS-line mapping of FTO/Bi-TiO<sub>2</sub>/(mp-TiO<sub>2</sub>/ZrO<sub>2</sub>) + MAPbI<sub>3</sub>/AV-C (a) artificially colored cross sectional SEM graph of device (b, c) line profile of all elements (d) EDS line scanning profile of each element across the device from bottom-to-top (e) respective EDS spectrum

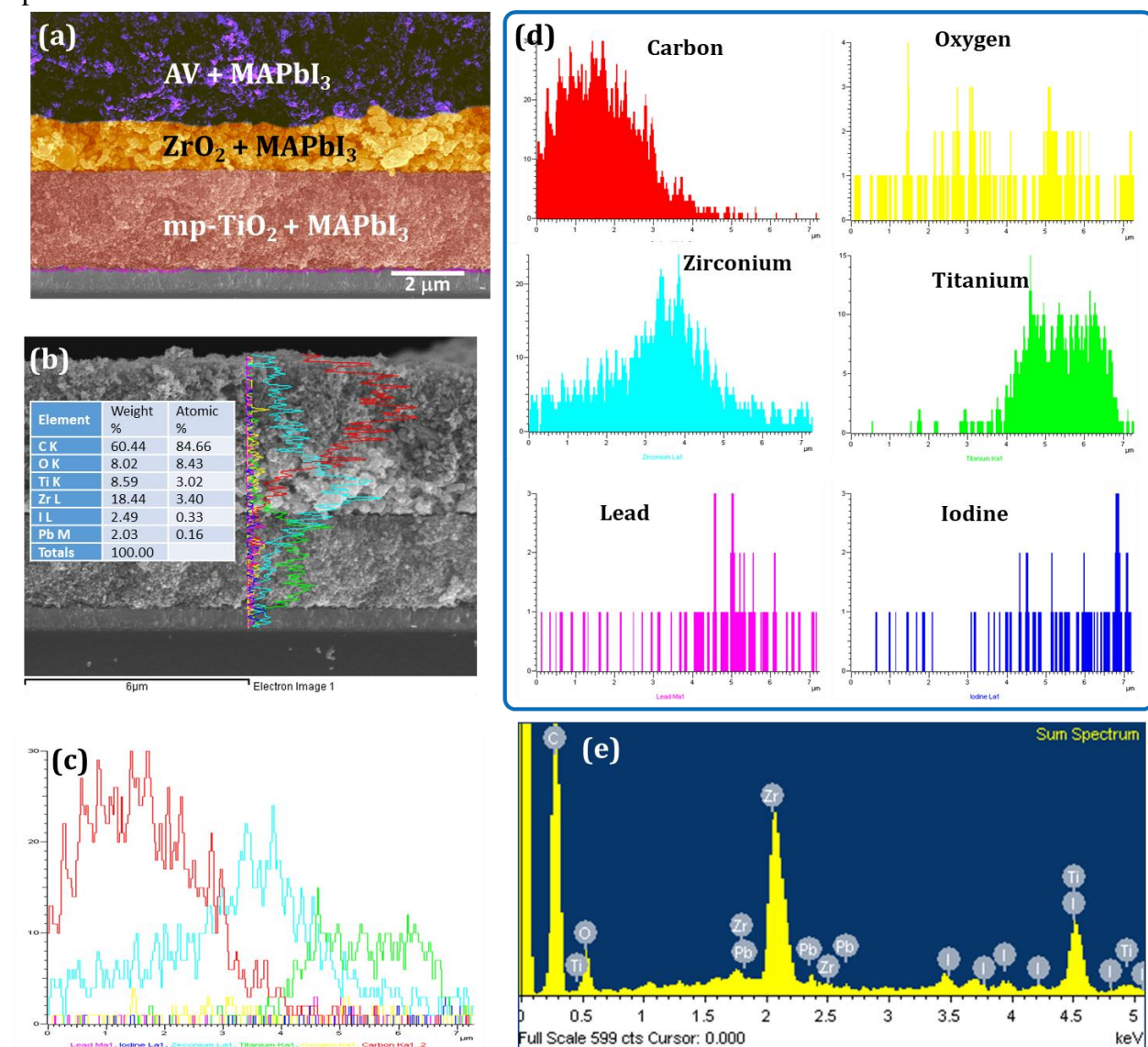




**Fig. S-8** J-V characteristics of commercial carbon based fully printable PSC. Inset shows the photovoltaic parameters extracted from the J-V curve.

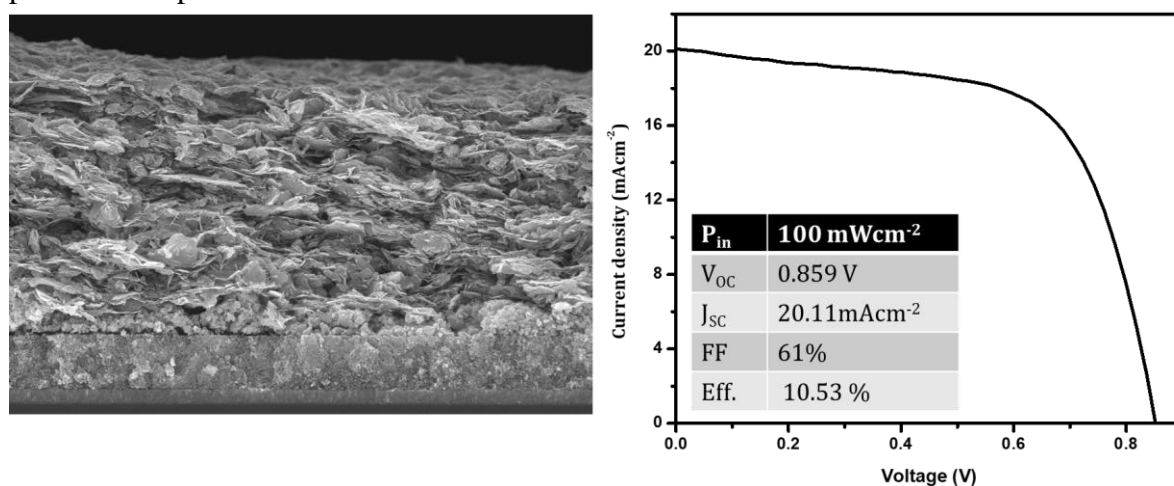


**Fig. S-9** Cross-sectional SEM image of conventional spiro-MeOTAD based PSC.

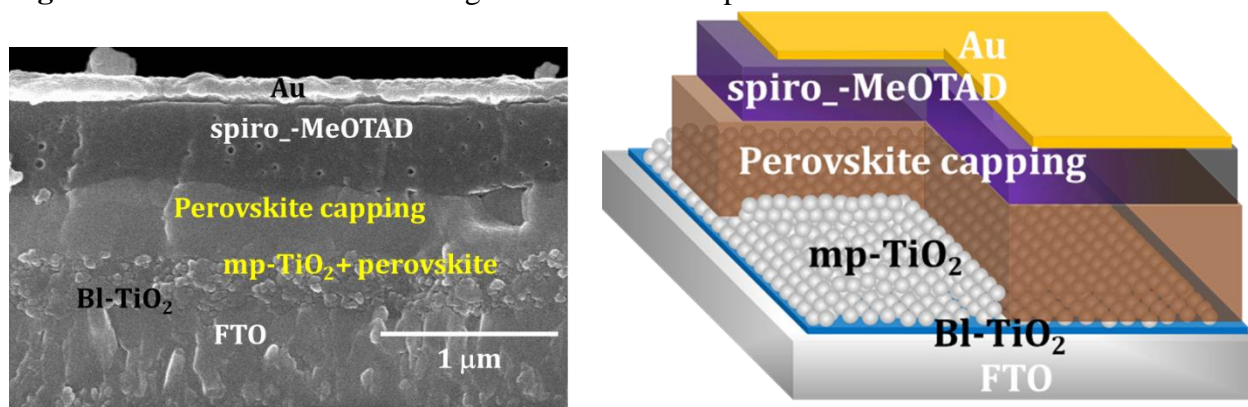




**Fig. S-10** Solid state impedance spectroscopy (ssIS) (a) Nyquist plot of the AV-C and commercial colloidal carbon based PSCs recorded under illumination at 0.8 V bias. The inset shows the equivalent circuit used for the analysis.

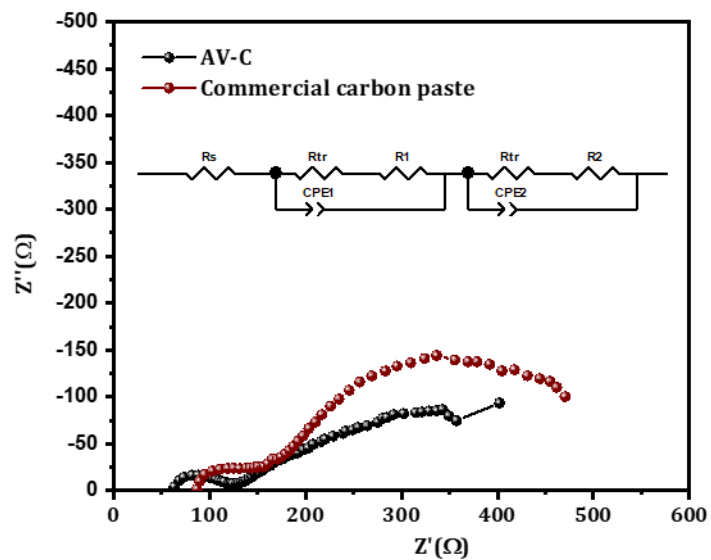


**Fig. S-11** Optical images of homemade humidity chamber (A) 37% humidity (B) 98% Humidity.

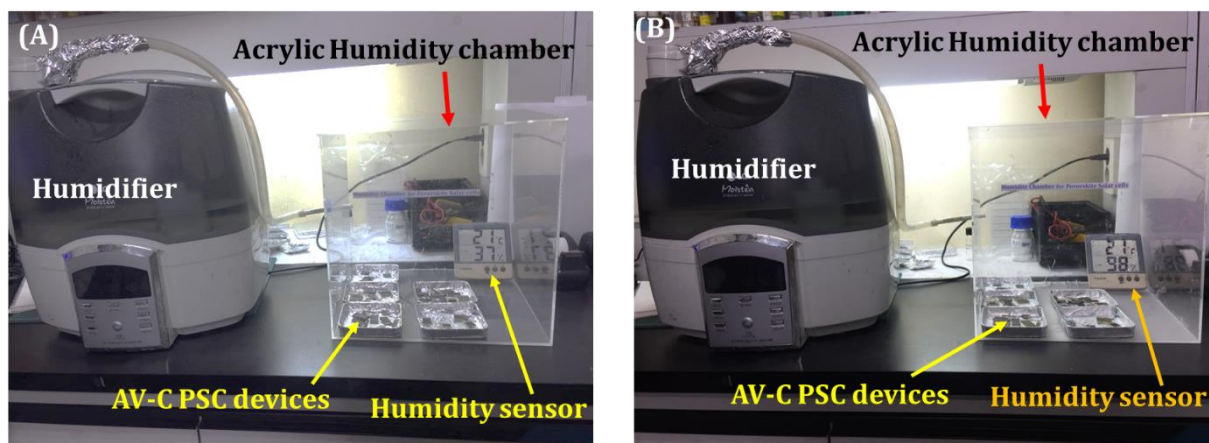


**Fig. S-12** Ambient air-stability of spiro-MeOTAD and AV-C based PSCs stored under ambient condition with 65 % RH. Commercial carbon based device stability has been given for comparison.

